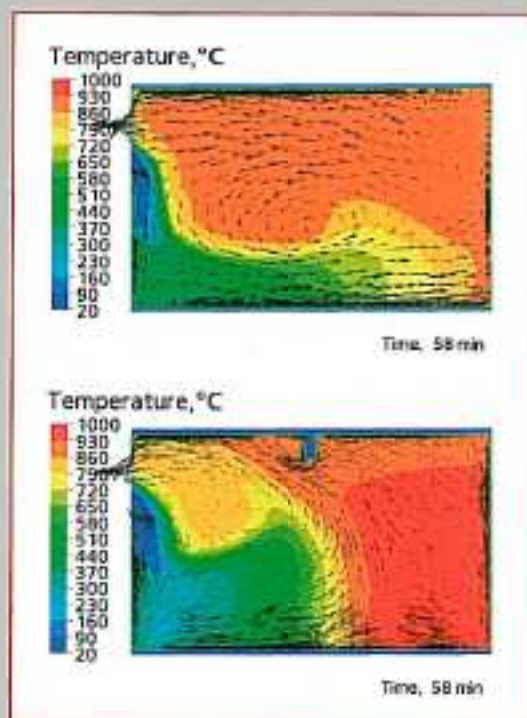


Proceedings of International Conference  
Prague, 19–20 February 2009

## APPLICATIONS OF STRUCTURAL FIRE ENGINEERING



Czech Technical University in Prague

PAULO PIRO  
PORTUGAL

Proceedings  
of International Conference  
in Prague, 19-20 February 2009

**APPLICATIONS  
OF STRUCTURAL FIRE ENGINEERING**



---

[eurofiredesign.fsv.cvut.cz](http://eurofiredesign.fsv.cvut.cz)  
Czech Technical University in Prague

**Proceedings of International Conference  
Applications of Structural Fire Engineering**  
hold during the Czech Presidency of the Council of the EU  
in Prague, 19-20 February 2009  
[eurofiredesign.fsv.cvut.cz](http://eurofiredesign.fsv.cvut.cz)

The preparation of the Proceedings was supported by the research centre of the Ministry of education, youth and sports CIDEAS No. 1M0579 and the Research plan Sustainable construction No. 6B40770005. The illustrative figures on the cover prepared by Nuno R.R. Almeida represent the opportunity of colleagues from Czech Technical University in Prague, University in Coimbra and Slovak Technical University in Bratislava to work on the seventh large fire test in Cardington.

Ed. Wald F., Kalleroová P., Chloubá J.  
ISBN 978-80-01-04266-3

Print Pražská technika, Czech Technical University in Prague  
January 2009, 200 copies

## DECOMPOSITION OF INTUMESCENT COATINGS: COMPARISON BETWEEN NUMERICAL METHOD AND EXPERIMENTAL RESULTS

Luís M.R. Mesquita<sup>a</sup>, Paulo A.G. Piloto<sup>a</sup>, Mário A.P. Vaz<sup>b</sup> and Tiago M.G. Pinto<sup>a</sup>

<sup>a</sup> Polytechnic Institute of Bragança, Applied Mechanics Department, Portugal.

<sup>b</sup> University of Porto, Faculty of Engineering, Portugal.

### INTRODUCTION

Passive fire protection materials insulate steel structures from the effects of the elevated temperatures that may be generated during fire. They can be divided into two types, non-reactive, of which the most common types are boards and sprays, and reactive, being intumescent coatings an example. They are available as solvent or water based systems applied up to approximately 3[mm]. One problem associated with the use of such systems is the adhesion of the charred structure to the steel element during fire and upon it. It is very important that the char remains in the steel surface to insure the fire protection.

The intumescent chemistry has changed little over the past years and almost all coatings are largely based on the presence of similar key components. The chemical compounds of intumescent systems are classified in four categories: a carbonisation agent, a carbon rich polyhydric compound that influences the amount of char formed and the rate of char formation; an acid source, a foaming agent, which during their degradation release non-flammable gases such CO<sub>2</sub> and NH<sub>3</sub>, [1].

Activated by fire or heat, a sequential chemical reaction between several chemical products takes place. At higher temperatures, between 200-300 [°C], the acid reacts with the carboniferous agent. The formed gases will expand, beginning the intumescence in the form of a carbonaceous char. Different models handle the intumescent behaviour with char forming polymers as a heat and mass transfer problem. Other existing models provide a suitable description regarding the intumescence and char formation using kinetic studies of thermal degradation, accounting the complex sequence of chemical reactions, thermal and transport phenomenon, [2]-[5].

Due to the thermal decomposition complexity of intumescent coating systems, the models presented so far are based on several assumptions, being the most relevant the consideration of one-dimensional heat transfer through material, temperature and space independent thermal properties and the assumption of a constant incident heat flux where the heat losses by radiation and convection are ignored, [3]. Some authors also assume that the thermochemical processes of intumescence occur without energy release or energy absorption, [6]. Results show that the insulation efficiency of the char depends on the cell structure and the low thermal conductivity of intumescent chars result from the pockets of trapped gas within the porous char which act as a blowing agent to the solid material.

The authors, in a previous work, considering the results obtained from coated steel plates tested in a cone calorimeter studied the intumescence as one homogenous layer. The steel temperature variation was considered and with the intumescence thickness time variation an inverse one-dimensional heat conduction problem (IHCP) was applied to determine the intumescence effective thermal conductivity and thermal resistance [7].

This work presents an experimental study to assess the performance of water-based intumescent paints used as a passive fire protection material. These tests were performed in a cone calorimeter, in steel plates coated with two different paints, three dry film thicknesses and considering two different radiant heat fluxes. During tests, among other quantities, the steel temperature, the intumescence mass loss and thickness variation were measured. A numerical model is also presented to study the intumescence behaviour. The paint thermal decomposition numerical model is based on the conservation equation of energy, mass and momentum.

### 1. EXPERIMENTAL TESTS PERFORMED IN THE CONE CALORIMETER

To assess the performance of two commercial water-based intumescent paints a set of experimental

tests was performed in a cone calorimeter, see Fig. 1 and Fig. 2. The steel plates are 100 [mm] squared and 4, 6 [mm] thick, coated in one side with different dry film thicknesses and tested in a cone calorimeter as prescribed by the standard ISO5660, [8]. Temperatures are measured by means of four thermocouples, type k, welded at the plate in the heating side and at the opposite side, at two different positions. The samples were weighted before and after of being coated allowing for the initial coating mass. The dry thickness was also measured in 16 different points, being the mean values and the standard deviation presented in the Fig. 1.

| Specimen     | Initial mass [g] | Final mass [g] | Coating mass [g] | Paint (mass) [g/100] | Paint (area) [cm <sup>2</sup> ] | Paint (thick) [mm] |
|--------------|------------------|----------------|------------------|----------------------|---------------------------------|--------------------|
| B 35 4 0.5 1 | 367.71           | 375.35         | 7.64             | 571                  | 100                             | 11.5               |
| B 35 4 0.5 2 | 365.58           | 374.80         | 9.22             | 70.6                 | 18.5                            |                    |
| B 35 4 0.5 3 | 364.55           | 373.95         | 9                | 600                  | 44.5                            |                    |
| B 35 4 1.5 1 | 355.53           | 359.10         | 3.57             | 1310                 | 78.2                            |                    |
| B 35 4 1.5 2 | 353.87           | 351.47         | 2.40             | 1320                 | 58.1                            |                    |
| B 35 4 1.5 3 | 354.88           | 350.50         | 5.38             | 1508                 | 68.5                            |                    |
| B 35 4 2.5 1 | 355.44           | 409.93         | 54.49            | 2546                 | 90.0                            |                    |
| B 35 4 2.5 2 | 356.74           | 409.12         | 52.38            | 2462                 | 89.0                            |                    |
| B 35 4 2.5 3 | 356.48           | 407.77         | 51.29            | 2310                 | 83.7                            |                    |
| B 75 4 0.5 1 | 362.92           | 371.94         | 9.02             | 581                  | 10.0                            |                    |
| B 75 4 0.5 2 | 366.00           | 375.97         | 9.97             | 662                  | 15.0                            |                    |
| B 75 4 0.5 3 | 367.42           | 377.47         | 10               | 611                  | 11.3                            |                    |
| B 75 4 1.5 1 | 366.71           | 378.11         | 11.40            | 1540                 | 10.3                            |                    |
| B 75 4 1.5 2 | 364.63           | 370.63         | 6.00             | 1551                 | 61.3                            |                    |
| B 75 4 1.5 3 | 373.29           | 374.69         | 1.40             | 1554                 | 74.3                            |                    |
| B 75 4 2.5 1 | 384.21           | 389.66         | 5.45             | 2335                 | 11.1                            |                    |
| B 75 4 2.5 2 | 364.24           | 401.19         | 36.95            | 2423                 | 50.4                            |                    |
| B 75 4 2.5 3 | 364.91           | 404.57         | 39.66            | 2499                 | 126                             |                    |
| B 75 4 3.5 1 | 426.00           | 537.09         | 111.09           | 537                  | 28.2                            |                    |
| B 75 4 3.5 2 | 425.91           | 571.74         | 145.83           | 1870                 | 100                             |                    |
| B 75 4 3.5 3 | 431.67           | 554.85         | 123.18           | 361                  | 65.9                            |                    |
| B 75 4 3.5 4 | 429.04           | 579.00         | 150.00           | 7610                 | 75.4                            |                    |
| A 35 4 0.5 1 | 363.77           | 375.36         | 11.59            | 571                  | 47.1                            |                    |
| A 35 4 0.5 2 | 363.81           | 375.35         | 11.54            | 571                  | 58.1                            |                    |
| A 35 4 0.5 3 | 364.54           | 375.19         | 10.65            | 571                  | 68.4                            |                    |
| A 35 4 1.5 1 | 361.10           | 367.74         | 6.64             | 1670                 | 17.2                            |                    |
| A 35 4 1.5 2 | 362.17           | 368.06         | 5.89             | 1619                 | 72.2                            |                    |
| A 35 4 1.5 3 | 361.30           | 365.43         | 4.13             | 1450                 | 84.3                            |                    |
| A 35 4 2.5 1 | 367.81           | 407.77         | 39.96            | 2570                 | 149                             |                    |
| A 35 4 2.5 2 | 365.81           | 407.83         | 42.02            | 2508                 | 172                             |                    |
| A 35 4 2.5 3 | 365.05           | 405.77         | 40.72            | 2558                 | 170                             |                    |
| A 75 4 0.5 1 | 365.48           | 374.36         | 8.88             | 549                  | 40.3                            |                    |
| A 75 4 0.5 2 | 361.34           | 371.50         | 10.16            | 581                  | 61.1                            |                    |
| A 75 4 0.5 3 | 368.44           | 377.85         | 9.41             | 572                  | 68.0                            |                    |
| A 75 4 1.5 1 | 366.74           | 382.67         | 15.93            | 1581                 | 83.7                            |                    |
| A 75 4 1.5 2 | 371.11           | 386.26         | 15.15            | 1551                 | 87.0                            |                    |
| A 75 4 1.5 3 | 364.87           | 381.73         | 16.86            | 1620                 | 98.7                            |                    |
| A 75 4 2.5 1 | 366.87           | 407.71         | 40.84            | 2590                 | 122                             |                    |
| A 75 4 2.5 2 | 365.11           | 406.00         | 40.89            | 2591                 | 135                             |                    |
| A 75 4 2.5 3 | 370.60           | 410.77         | 40.17            | 2550                 | 107                             |                    |
| A 75 4 3.5 1 | 427.27           | 537.09         | 109.82           | 536                  | 28.2                            |                    |
| A 75 4 3.5 2 | 426.65           | 567.71         | 141.06           | 1870                 | 100                             |                    |
| A 75 4 3.5 3 | 432.80           | 550.58         | 117.78           | 361                  | 65.9                            |                    |
| A 75 4 3.5 4 | 435.71           | 564.28         | 128.57           | 7610                 | 75.4                            |                    |

Fig. 1. Set of experimental tests. Reference: Paint/Heat Flux/Steel Thick./Dry Thick./Test N°.



Fig. 2. Coated steel plates, with fixed thermocouples. Tested samples at 35 [kW/m<sup>2</sup>] and at 75 [kW/m<sup>2</sup>]. Reference and position of the thermocouples.

Between the steel plate and the sample older two silicate plates were used to put the specimen in place and also a thermocouple was placed to measure its temperature variation. The distance between the sample surface and the heater remained unchanged, at approximately 60 [mm], which means that with the increasing intumescence the top of the sample came closer to cone surface. Due to the large amount of results, only a set of samples will be referenced in this paper.

## 1.1 Experimental Results

The temperature evolution in a steel plate without protection was also tested to attain the efficiency of this fire protection. The measured temperatures are presented in the Fig. 3 for a radiant heat flux of 35 [KW/m<sup>2</sup>] and then resetting the cone to 75 [KW/m<sup>2</sup>].

Fig. 4 represents the mass loss of each sample and shows a variation almost linear with time mainly for a heat flux of 35 [kWm<sup>-2</sup>].

Using discrete frames obtained from digital camera during tests and by image processing techniques using Matlab, the intumescence development was measure over time. Fig. 5 presents the intumescent development (free boundary L(t)) for specimens with paint A and B, different thicknesses and radiant heat fluxes.

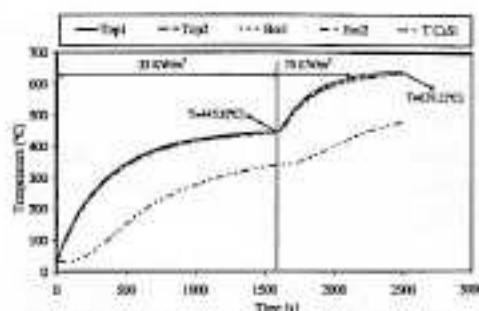


Fig. 3. Measured temperature in the steel plate without protection.

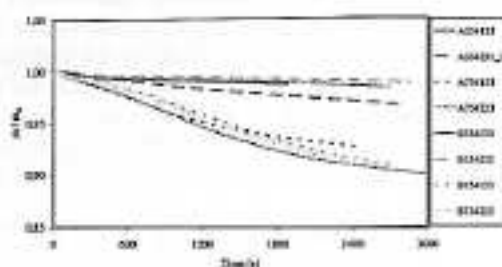


Fig. 4. Measured mass loss with time.

Higher intumescence may be noticed in sample right region coincident to the thermocouples wire position responsible for coating accumulation. The presented values are mean values determined from four central measures.

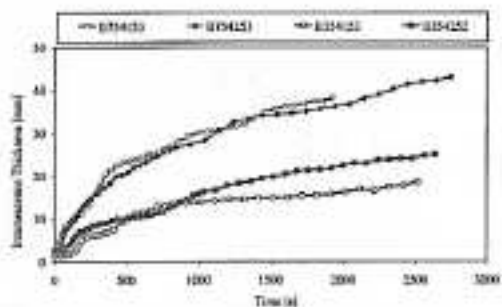
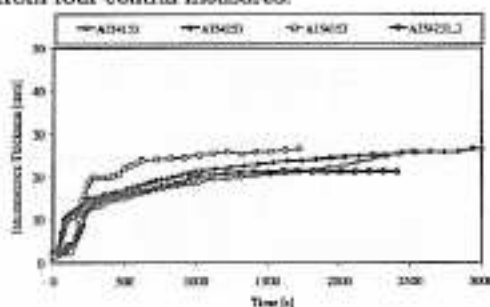


Fig. 5. Intumescence thickness mean values of four central measurements.

The figures shown that for the lower heat flux the intumescence becomes stable, but for the higher it continues to increase. Coating A presents a higher expansion at the initial stage compared to the coating B. For longer exposure periods of exposure coating B continues to expand.

The steel temperature profiles and temperatures at the middle of the silicate plates are reported in Fig. 6 and Fig. 7. Measured values from the thermocouples welded on the bottom of the plate are very close to the temperatures at the top. For the same heat flux, the time to reach a same temperature increases with the increase of the dry thickness.

The behaviour is very similar for both coatings, but for all cases the time to reach, for example a temperature of 200 [°C] is always higher when the paint B is used. For these conditions it gives an improved fire protection.

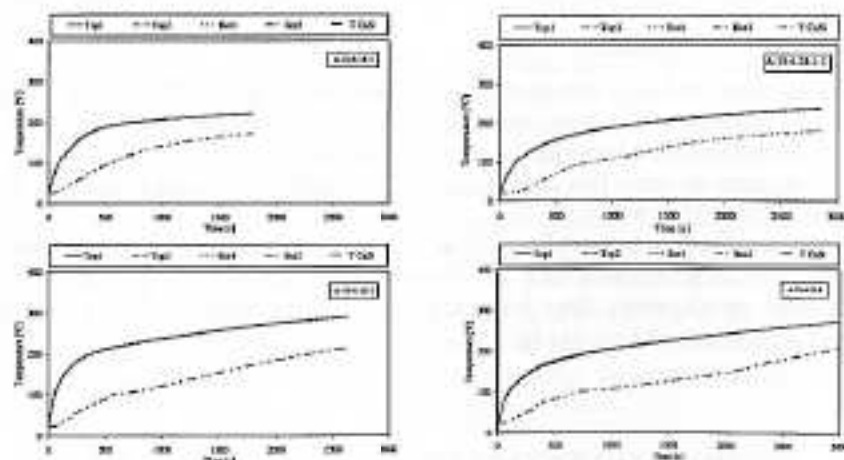


Fig. 6. Temperature variation of steel and silicate plates for coating A.



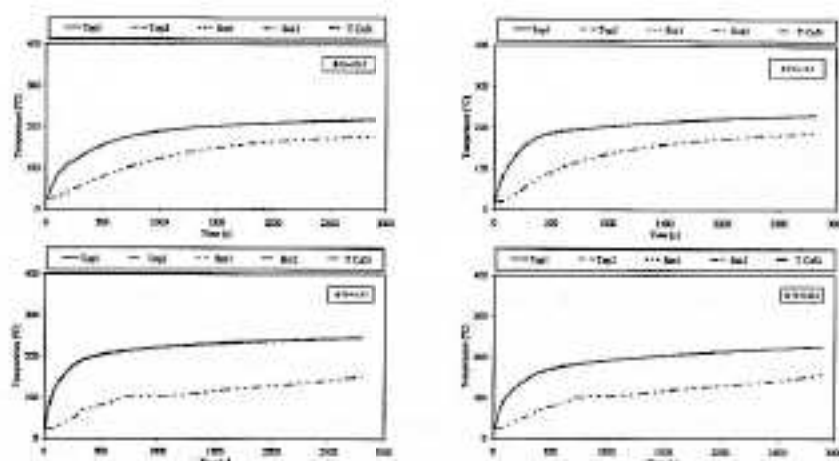


Fig. 7. Temperature variation of steel and silicate plates for coating B.

## 2 MATHEMATICAL MODEL OF THE INTUMESCENCE BEHAVIOUR

The problem to determine the temperature field in an intumescent material involves the solution of a phase transformation problem with two or more moving boundaries that characterize its state, initial, softened and carbonaceous char. Different methodologies can be found in the literature to model the thermal decomposition of a polymer or polymer based materials. The methodology followed in this work was to consider that the decomposition occurs not only at the outside surface but also inside, for temperatures above the pyrolysis temperature,  $T_p$ . In this case the moving boundary regression rate must be determined considering the motion of all domain. This strategy implies that a mass diffusion term needs to appear in the energy equation due its motion. This term was disregarded due to the small thickness of the virgin layer for this types of applications, about 1-3 [mm].

Considering a first order reaction, the mass loss is given by

$$\dot{m}(T(x,t)) = \frac{\partial \rho_s}{\partial t} = -\rho_s A_0 e^{-\frac{E_0}{RT(x,t)}} \quad \text{for } T \geq T_p \quad (1)$$

where  $\dot{m}$  is the local mass loss [ $\text{kg} \cdot \text{m}^{-3} \cdot \text{s}^{-1}$ ],  $T(x,t)$  is the temperature at point  $x$  at instant  $t$ ,  $A_0$  is the pre exponential factor [ $\text{s}^{-1}$ ],  $E_0$  the activation energy [ $\text{J} \cdot \text{mol}^{-1}$ ], and  $R$  the universal gas constant [ $\text{J} \cdot \text{mol}^{-1} \cdot \text{K}^{-1}$ ]. The position of the moving boundary is obtained by summing all the mass loss and dividing by the specific mass.

The energy equation for the steel and virgin layers is based on the one-dimensional conduction heat equation.

The conservation equation for the solid virgin material phase is given by

$$\frac{\partial \rho_s V_s}{\partial t} = -\dot{w}_s^v V_s \quad (2)$$

Where  $\dot{w}_s^v$  represents the destruction rate of virgin material per unit volume, originated by the thermal decomposition. The virgin material decomposition produces a fraction of gas, equal to the porosity,  $\phi$ , and a solid char fraction equal to  $(1-\phi)$ .

The formation rate of char and gas mass is:

$$\dot{w}_{\text{gas}}^p = -\left(1 - \frac{\rho_c}{\rho_s}\right) \chi \rho_s A \frac{ds(t)}{dt} \quad \dot{w}_{\text{char}}^p = -\left[1 - \left(1 - \frac{\rho_c}{\rho_s}\right) \chi\right] \rho_s A \frac{ds(t)}{dt} \quad (3)$$

$\chi$  represents the fraction of the bulk density difference between the virgin and char materials that is converted to gas. In this study the value used was  $\chi = 0.66$ , [9].

The conservation of gas mass equation is given by eq. (4).

$$\frac{\partial(\rho_s \varphi)}{\partial t} + \frac{\rho_s \varphi}{V} \frac{\partial V}{\partial t} + \frac{\partial \dot{m}_g}{\partial x} = 0 \quad (4)$$

In the previous equation  $\partial V/\partial t$  represents the intumescence rate. The gas mass flux,  $\dot{m}_g$ , is calculated accordingly to Darcy's law and it is assumed that the gases present in the intumescent material behave as a perfect gas. The thermodynamic properties are related by the ideal gas law and, assuming that the gas is a mixture of 50wt%CO<sub>2</sub> and 50wt%H<sub>2</sub>O, the generated gas molar mass used in the model  $M_g$  is 31[g/mol].

The conservation of gas mass equation with the Darcy's and the ideal gas laws combined can be used to give a differential equation for the pressure inside the intumescence. In the numeric calculations, the intumescence rate is assumed to be known, provided by the experimental results, so the pressure calculation is disregarded being assumed that the internal pressure is constant and equal to the atmospheric pressure. An energy equation for the conservation of energy within the intumescence zone can be obtained by combining the energy equation for the gases with that of the solid char material. The equation for the conservation of energy per unit bulk volume can be written as:

$$(\rho C_p)_{eff} \frac{\partial T}{\partial t} + \frac{\partial}{\partial x} (\dot{m}_g T_g C_{p_g}) = \frac{\partial}{\partial x} \left( k_{eff} \frac{\partial T}{\partial x} \right) - C_p T \frac{\partial \rho}{\partial t} - (\rho C_p)_{eff} \frac{T}{V} \frac{\partial V}{\partial t} \quad (5)$$

where  $(\rho C_p)_{eff} = \varphi \rho_s C_{p_s} + (1 - \varphi) \rho_g C_{p_g}$  and  $k_{eff} = \varphi k_s + (1 - \varphi) k_g$ .

The effective thermal conductivity for the intumescence bulk material, including gas and char, is equal to the thermal conductivity of the gas per unit bulk volume, plus that of the solid material. The same thing applies to the effective heat capacity.

In the steel plate back surface it is assumed an adiabatic boundary condition and at the boundary steel/virgin layers it is assumed a perfect thermal contact. At the moving front, the boundary conditions are:

$$\begin{aligned} k_s \frac{\partial T}{\partial x} &= \varepsilon \dot{q}_r - \varepsilon \sigma (T^4 - T_c^4) - h_c (T - T_c) & \text{for } T(s(t), t) < T_r \\ k_s \frac{\partial T}{\partial x} - k_c \frac{\partial T}{\partial x} &= Q_n & \text{for } T(s(t), t) = T_r \end{aligned} \quad (6)$$

In which  $Q_n$  is the heat flux due to the endothermic decomposition of the virgin material, given by  $Q_n = -h_p \rho_s \dot{s}(t)$ , where  $h_p$  represents the decomposition enthalpy. A wide range of values are reported in the literature for the heat of pyrolysis and go from a few units to units of millions. The value used in the calculations was 50 [J/kg].

The intumescent coating specific mass was measured by the pycnometer method given a value of 1360 and 1250 [kg/m<sup>3</sup>] for the virgin coating and a value of 692.4 and 450 [kg/m<sup>3</sup>] for the char material, for paints A and B, respectively. Steel properties are assumed constant, with a specific heat value of 600 [J/kgK] and a specific mass equal to 7850 [kg/m<sup>3</sup>]. The intumescent coating specific heat was considered constant and equal to 1000 [J/kgK].

The mathematical model is based on the following major simplifying assumptions: there is no heat between gas and char, the thermophysical properties and the pressure at both layers are constant.

The solution method was implemented in a Matlab routine using the Method Of Lines (MOL), [10], and the integrator *ode15s* to solve the set of ordinary differential equations.

The temperature field is determined by the steel and virgin energy equations. When the front reaches the pyrolysis temperature, equal to 250 [°C], starts to decompose and to move. Then the moving front rate is determined and the intumescence forms. The position the free boundary is set equal to the experimental results and the intumescence temperature field is determined. In each time step the virgin and char layers are remeshed.

The input parameters are listed as follows:  $k_s = 0.5 \text{ W m}^{-1} \text{ K}^{-1}$ ;  $k_c = 0.1 \text{ W m}^{-1} \text{ K}^{-1}$ ;  $C_{p_s} = 2600 \text{ J kg}^{-1} \text{ K}^{-1}$ ;  $C_{p_c} = 3000 \text{ J kg}^{-1} \text{ K}^{-1}$ ;  $h_c = 20 \text{ W m}^2 \text{ K}^{-1}$ ;  $\varepsilon = 0.92$ ;  $T_p = 525 \text{ K}$ ;  $A_0 = 4.67 \text{ e}^{12} \text{ s}^{-1}$ .



Two case studies are presented in Fig. 8 and Fig. 9. In the first one the steel temperature variation and the moving front position are determined based on a value of the activation energy equal to  $E_0 = 125 \text{ KJmol}^{-1}$ . The numerical results follow reasonably well the experimental values. The major differences occur at intermediate times probably because a transition state of molten polymer was not considered.

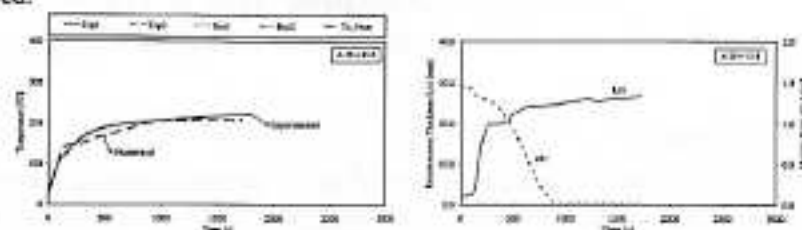


Fig. 8. Comparison of measured and computed steel temperatures and position of the moving front,  $E_0 = 125 \text{ KJmol}^{-1}$ .

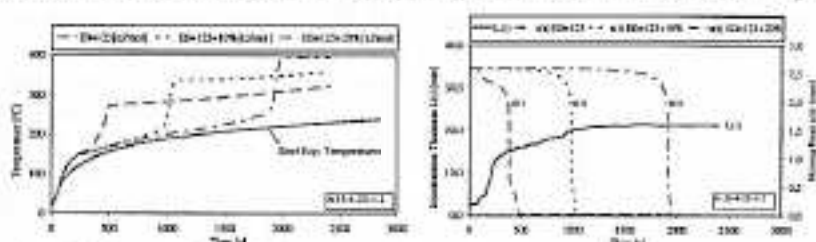


Fig. 9. Influence of the activation energy in the steel temperature and in the moving front.

Both the determined steel temperatures and the moving front are strongly dependent on the activation energy that defines the amount of mass loss of virgin paint, as presented in Fig. 9. It must be said that the value used in the simulations was obtained from the literature, but the correct value of both paints are needed. The reaction kinetics parameters can be obtained from thermogravimetric analysis.

#### ACKNOWLEDGMENTS

The authors acknowledge the financial support from the Portuguese Science and technology Foundation, project PTDC/EME-PME/64913/2006, "Assessment of Intumescent Paint Behaviour for Passive Protection of Structural Elements Submitted to Fire Conditions", and fellowship SFRH/BD/28909/2006. The authors acknowledge also the contribution from the paints producers: CIN, Nullifire.

#### REFERENCES

- [1] Duquesne, S.; Bourbigot, S.; Delobel, R., "Mechanism of fire protection in intumescent coatings", European Coatings Conference: Fire Retardant Coatings II, Berlin, 2007.
- [2] Staggs J. E. J., "A discussion of modelling idealised ablative materials with particular reference to fire testing", *Fire Safety Journal*, Vol. 28, 47-66, 1997.
- [3] Moghtaderi B., Novozhilov V., Fletcher, D., Kent J. H., "An integral model for the transient pyrolysis of solid materials" *Fire and Materials*, Vol. 21, 7-16, 1997.
- [4] Lyon R. E., "Pyrolysis kinetics of char forming polymers", *Polymer Degradation and Stability*, N° 61, pp. 201-210, 1998.
- [5] Jia F., Galea E. R., Patel M. K., "Numerical Simulation of the Mass Loss Process in Pyrolyzing Char Materials", *Fire And Materials*, N° 23, 71-78, 1999.
- [6] Kuznetsov, G. V., Rudzinskii, V. P., "Heat transfer in intumescent heat- and fire-insulating coatings", *Journal of Applied Mechanics and Technical Physics*, Vol. 40, No. 3, 1999.
- [7] Mesquita, L.M.R.; Piloto, P.A.G.; Vaz, M.A.P.; Pinto, T., "Numerical Estimation For Intumescent Thermal Protection Using One-Dimensional IHCP", WCCM8-ECCOMAS2008, ISBN: 978-84-96736-55-9, Venice, Italy, June 30 - July 5, 2008.
- [8] ISO 5660-1:2002, Reaction-to-fire tests - Heat release, smoke production and mass loss rate. Part 1: Heat release rate (cone calorimeter method), International Organization for Standardization, 2002.
- [9] C. Lantierberger, A Generalized Pyrolysis Model for Combustible Solids, Ph.D. thesis, University of California at Berkeley, Berkeley, CA, 2007.
- [10] Wouwer A.V, Saez P., and W. E. Schiesser, "Simulation of Distributed Parameter Systems Using a Matlab-Based Method of Lines Toolbox: Chemical Engineering Applications", *Ind. Eng. Chem. Res.* 2004, 43, 3469-3477.



Applications of Structural Fire Engineering  
19 - 20 February 2009

# YOUNG RESEARCHER AWARD

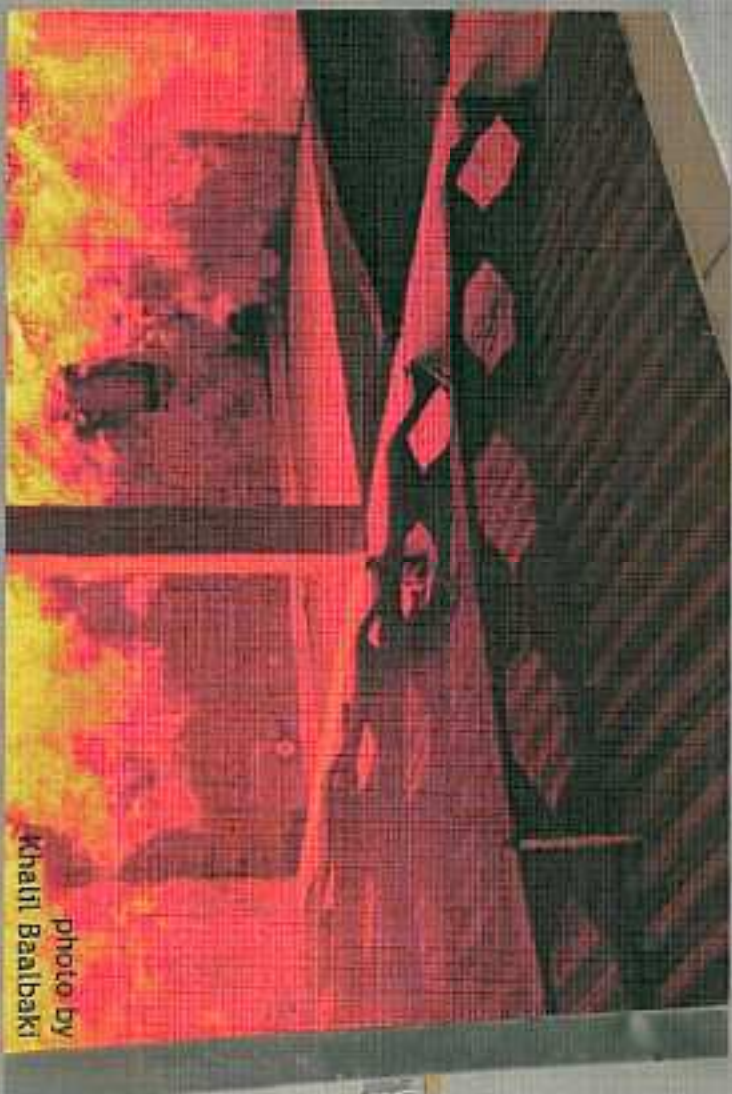


photo by  
Khalil Baalbaki

to Mr/Ms

*Menawida Luis*

*prof.* Ing. Frankish Wald, PhD.

*prof. Ing. Ian Burgess, PhD.*